World Journal of Microbiology and Biotechnology (2022) 38:14
https://doi.org/10.1007/s11274-021-03193-1

ORIGINAL PAPER

Enhancing the production of physiologically active vitamin D_3 by engineering the hydroxylase CYP105A1 and the electron transport chain

Bing Fu[1,2] · Qian Ren[1] · Jian Ma[1] · Qingwei Chen[1] · Qili Zhang[1] · Ping Yu[1]

Received: 27 July 2021 / Accepted: 17 November 2021 / Published online: 8 December 2021

Abstract
In this study, the conversion of vitamin D_3 (VD_3) to its two active forms 25(OH)VD_3 and 1α, 25$(OH)_2VD_3$ was carried out by engineering the hydroxylase CYP105A1 and its redox partners Fdx and Fdr. CYP105A1 and Fdx–Fdr were respectively expressed in *E. coli* BL21(DE3) and purified. The electron transport chain Fdx–Fdr had higher selectivity for the coenzyme NADH than NADPH. HPLC analysis showed that CYP105A1 could hydroxylate the C25 and C1α sites of VD_3 and convert VD_3 to its active forms. Finally, a one-bacterium-multi-enzyme system was constructed and used in whole-cell catalytic experiments. The results indicated that 2.491 mg/L of 25(OH)VD_3 and 0.698 mg/L of 1α, 25$(OH)_2VD_3$ were successfully produced under the condition of 1.0% co-solvent DMSO, 1 mM coenzyme NADH and 35 g/L biocatalyst loading. This study contributes to a basis for the industrial production of active VD_3 in future.

Keywords Synthetic biology · Active VD_3 · Hydroxylase · Redox partner · Whole cell catalysis

Introduction

Vitamin D_3 (VD_3), also known as "the sunshine vitamin," is a fat-soluble vitamin and hormone precursor that plays an important role in the metabolism of calcium and phosphorus. It is also an essential substance for the growth and reproduction of humans and animals (DeLuca 1982; Pike 1991). However, VD_3 has no physiological activity. In mammals, vitamin D_3 is converted to active forms when hydroxylation occurs at the C1α or C25 site in the parent nuclear structure of VD_3 through the hydroxylation of CYP450 enzymes in liver and kidney cells (Brenza and DeLuca 2000; Kang et al. 2006), including 1α(OH)VD_3, 25(OH)VD_3, and 1α, 25$(OH)_2VD_3$. The most active form is 1α, 25$(OH)_2VD_3$ (Bury et al. 2001; Koyama et al. 1998). The metabolic process of VD_3 in the human body involves a two-step hydroxylation reaction (DeLuca and Schnoes 1983), which is shown in Fig. 1.

Active vitamin D_3 can be produced through chemical synthesis and microbial transformation. The chemical synthesis method is unsuitable for industrial production because of its disadvantages, such as multiple and complex steps, unstable properties, complex structures, difficulty in separation and purification, a high preparation cost, low synthesis efficiency, and serious pollution (Kametani and Furuyama 1987). Given an increasing demand for active VD_3, an efficient method that can replace chemical synthesis and facilitate its industrial production is urgently needed. The microbial transformation has a low cost and high stereoselectivity and causes low environmental pollution, greatly shortening the reaction steps of chemical synthesis. Moreover, the catalytic reaction condition of biological enzymes is mild and has a good repeatability. It can facilitate automatic production of active VD_3 and has a wide application prospect (Kang et al. 2015).

C25 and C1α sites are the two main hydroxylation sites of VD_3 during microbial transformation for industrial processes. Researchers have screened bacteria, fungi and actinomycetes used in microbial transformation reactions (Fujii

✉ Ping Yu
yup9202@hotmail.com

[1] College of Food Science and Biotechnology, Zhejiang Gongshang University, 149 Jiaogong Road, Hangzhou 310035, Zhejiang Province, People's Republic of China

[2] College of Forestry Science and Technology, Lishui Vocational and Technical College, 357 Zhongshan Street North, Lishui 323000, Zhejiang Province, People's Republic of China

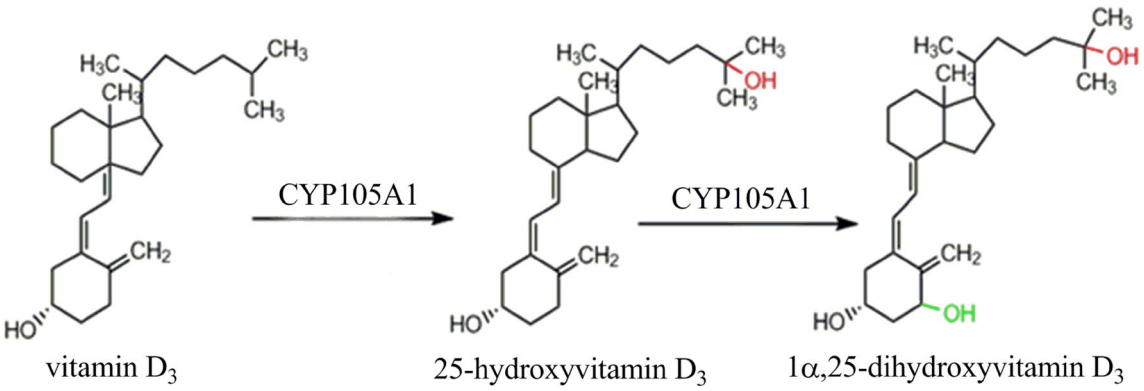

Fig. 1 Metabolic process of VD_3 in the human body

et al. 2009). *Pseudonocardia autotrophica* and *Stretomyces* are the most commonly found in applied studies. *Streptomyces* sp. is used to transform the 1α site of 25(OH)VD_3 to 1α, 25$(OH)_2VD_3$ (Sasaki et al. 1991). *P. autotrophica* ID 9302 and *Pseudonocardia* KCTC 1029BP are successively used in the transformation of 1α, 25$(OH)_2VD_3$ (Kang et al. 2015, 2006). *P. autotrophica* CGMCC5098 can be used in the transformation of 25$(OH)_2VD_3$ (Luo et al. 2017).

However, relying solely on screened wild-type strains for active VD_3 production has some disadvantages, such as low activity and many by-products. The reasons can be that vitamin D compounds are not the naturally preferred substrates for the hydroxylases of these strains and the normal physiological metabolism of the strains. Therefore, cloning key enzymes is necessary in enhancing the hydroxylation activity of VD_3 hydroxylase, particularly in obtaining the desired expression level and optimizing three-dimensional structures and active sites (Kawauchi et al. 1994).

In recent years, the wide application of genetic engineering technology in biotransformation and successive studies on the structure and function of CYP450 enzymes are the main reasons for the successful expression of VD_3 hydroxylases in *E. coli*, yeast, red coccus, and other engineered bacteria. Fast growth rate, easy operation, and improved conversion rate have been achieved (Imoto et al. 2011; Sakaki et al. 2011). Cytochrome p450su-1 (CYP105A1), derived from *Streptomyces griseolus*, is one of the most well-studied VD_3 hydroxylases (Sakaki et al. 2011; Sasaki et al. 1991; Sawada et al. 2004; Sugimoto et al. 2008). CYP105A1 not only has 25-hydroxylation activity towards VD_2 and VD_3, but also has 1α-hydroxylation activity towards 25(OH)VD_3 (Sawada et al. 2004). Hence, it is interesting to investigate the use of CYP105A1 to catalyze VD_3 to prepare physiologically active VD_3, 25(OH)VD_3 and 1α, 25$(OH)_2VD_3$.

The electron transport chain is critical to the catalytic efficiency of CYP450 enzymes, and a majority of CYP450s, including CYP105A1, must rely on one or more redox molecular chaperones (Fujii et al. 2009). The electron transport chains of CYP450s have several families. The ferredoxin (Fdx)–ferredoxin reductase (Fdr) electron transport chain, which belongs to the class I family, is currently a widely used artificial electron transport chain in bacteria (Fujii et al. 2009; Pham et al. 2013; Sawada et al. 2004). Other artificial electron transfer chains, such as putidaredoxin (Pdx)–putidaredoxin reductase (Pdr) and adrenodoxin (Adx)–adrenodoxin reductase (Adr), are also used in different microorganisms (Goñi et al. 2009; Hannemann et al. 2007).

This study aims to construct a one-bacterium-multi-enzyme system to convert VD_3 to its physiologically active forms, 25(OH)VD_3 and 1α, 25$(OH)_2VD_3$. In order to achieve this goal, the *CYP105A1* gene (GenBank accession Number M32238.1) derived from *S. griseolus* and the electron transport chain gene *Fdx–Fdr* (GenBank accession Number AB221118.1) dervied from *Acinetobacter* sp. OC4 were synthesized artificially and transformed into *E. coli* BL21 (DE3). The biological activities and hydroxylation processes of these key enzymes were analyzed. The results demonstrated that CYP105A1 from *S. griseolus* displayed a good hydroxylation activity towards VD_3. Moreover, the whole-cell-catalyzed VD_3 experiments in a multi-enzyme system were conducted to explore the effect of different factors on hydroxylation efficiency and to provide a basis for the industrial production of the physiologically active VD_3.

Materials and methods

Bacterial strains, plasmids, and growth conditions

All strains and plasmids used in the experiments are listed in Table 1. *Escherichia coli* DH5α was used as the host strain for constructing recombinant plasmids. The *E. coli* BL21 (DE3) strain was used as the expression host. Unless otherwise specified, the *E. coli* strain was cultured in Luria–Bertani (LB) medium (10 g/L peptone, 5 g/L yeast extract, and

Table 1 Strains and plasmids

Strains and plasmids	Primer sequences	Sources
Strains	*E. coli* DH5α	Invitrogen, USA
	E. coli BL21(DE3)	Invitrogen, USA
Plasmids	pET28a(+)	Invitrogen, USA
	pETDuet-1	Invitrogen, USA
Recombinant plasmids	pET28a-CYP105A1	This study
	pET28a-Fdx-Fdr	This study
	pETDuet-1-CYP105A1	This study
	pETDuet-1-CYP105A1-Fdx-Fdr	This study

10 g/L NaCl, pH 7.4) and incubated at 37 °C in a shake flask. All primer sequences used in this study are listed in Table 2 and were directly synthesized by Shanghai Sangon Biotech Co. Ltd, China. Isopropyl-*β*-D-thiogalactopyranoside (IPTG), peptone, yeast extract, NaCl, kanamycin, and ampicillin were purchased from BBI Co. Ltd, USA. Vitamin D_3, 25(OH)VD_3, and 1α, 25$(OH)_2VD_3$ were purchased from J&K Scientific Co. Ltd, China. The plasmid purification kit, DNA fragment purification kit, agarose gel DNA extraction kit, restriction endonucleases and T_4 DNA ligase were purchased from TaKaRa Co. Ltd, Japan.

Construction and transformation of recombinant plasmid based on pET28a(+)

The synthetic *CYP105A1* gene was ligated to the pET28a(+) expression vector after double digestion with two restriction endonucleases (*Bam*HI and *Xho*I), and the recombinant plasmid pET28a(+)-*CYP105A1* was obtained. The hydroxylase CYP105A1 belongs to the CYP450 enzyme family and requires electron transport chains (redox chaperones) to maintain hydroxylation reactions (Hannemann et al. 2007). According to the literature (Ahmed et al. 2014), Fdx–Fdr from *Acinetobacter* with good compatibility was selected as the electron transfer chain, and the whole gene was synthesized. In the same manner, the expression plasmid pET28a(+) was ligated to obtain the recombinant plasmid pET28a-*Fdx-Fdr*. The two recombinant plasmids pET28a(+)-*CYP105A1* and pET28a(+)-*Fdx-Fdr* were respectively transferred to *E. coli* BL21(DE3) competent cells. Positive clones were screened through verification in terms of plasmid size, double digestion, PCR, and sequencing and stored in glycerol tubes at − 80 °C.

Cultivation of recombinant *E. coli* cells

Recombinant *E. coli* BL21 (DE3) was incubated in LB medium containing 50 μg/mL kanamycin at 37 °C under good aeration. The transcription of the target gene under the *lac* promoter was initiated by the addition of IPTG at a concentration of 0.25 mM when the cell density (OD_{600}) reached 0.8. The recombinant *E. coli* BL21 (DE3) was gently shook at 25 °C, and the expression of target proteins were analyzed with SDS–PAGE.

Preparation of cytosolic fractions and SDS–PAGE analysis of the target proteins

After being induced for 24 h, the cultures were taken out and centrifuged at 12,000 rpm for 10 min. The obtained cells were resuspended in 5 mL of phosphate buffer (PBS, pH7.4) for ultrasonic treatment (work 6 s, pause 6 s, 150 W). The supernatant and precipitate of the resulting crushing solution were obtained through centrifugation (12,000 rpm, 10 min, 4 °C), and the precipitate was re-suspended with PBS buffer (pH7.4).

Approximately 20 μL of the supernatant and the precipitate were subjected to SDS–PAGE analysis, which was performed on a 12% running gel. Resolved proteins were visualized by staining with Coomassie brilliant blue G-250.

Purification of the target proteins

The target proteins were purified through Ni^{2+}-NTA column chromatography (Hefti et al. 2001; Janknecht et al. 1991). Cytosolic fractions prepared from each cell culture were applied to a Ni^{2+}- Sepharose column (Ni–NTA Sefinose™ Resin) equilibrated with binding/washing buffer (50 mM NaH_2PO_4, 300 mM NaCl, and 20 mM imidazole) at a flow rate of 1 mL/min. After the binding of the target proteins, the column was washed with the same buffer, and the

Table 2 Primer sequences used in this study

Genes	Primer names	Sequences	Restriction sites
CYP105A1	CYP105A1-F_1	5′-TCGCGGATCCGATGACCG ATACCGCCACGACGCCCC-3′	*Bam*HI
	CYP105A1-R_1	5′-CTTCAAGCTTTTACCAGGTGACCGGGAGTTCGTTGA-3′	*Hin*dIII
Fdr–Fdx	Fdrx–F_1	5′-TCGGCATATGCAAACAAT CGTCATCATTGGCGC-3′	*Nde*I
	Fdrx-R_1	5′-GCTTCTCGAGTTACATCTGAAACTCAGGCAGATGTA-3′	*Xho*I

histidine-tagged protein was eluted with elution buffer (50 mM NaH_2PO_4, 300 mM NaCl, and 250 mM imidazole, pH 8.0).

Biological activity analysis of the electron transport chain

The oxidation activity and preference of Fdr on NAD(P)H was evaluated using 2, 6-indophenol sodium dichloride (DCPIP), which is an oxidation–reduction indicator with a blue oxidation state (absorption peak at 600 nm) and colorless reduced state (absorption peak disappears at 600 nm) (Dean and Pocock 2004). The oxidation activity of Fdr to NAD(P)H and the preference of Fdr to NADH or NADPH can be evaluated according to the reduction rate of light absorption value at 600 nm. The reaction system (1.5 mL) included 200 µL of DCPIP, 50 µL of 200-fold-diluted purified enzyme solution Fdx–Fdr, 650 µL of PBS buffer at pH 7.2–7.4, and 100 µL of 10 mM NaCl solution. After the mixture was evenly mixed, 180 µL of the mixture was taken out and added to a 96-well plate, then 20 µL of 30 mM NADH was added to initiate the electron transfer reaction. The OD_{600} value change within 15 min was immediately measured with a microplate at an absorption wavelength of 600 nm, and the absorption change curve was recorded.

In the control group, 20 µL of 30 mM NADH solution was replaced with 20 µL of PBS buffer at pH 7.2–7.4. The NADPH control group was set up, and 20 µL of 30 mM NADH solution was replaced with 20 µL of 30 mM NADPH solution. The preferential selection of the electron transport chain Fdx–Fdr for NADH or NADPH was studied.

Cytochrome C was used in evaluating the activities of Fdx and Fdr. Cytochrome C is a protein containing ferric hemoglobin, which can receive electrons mediated by Fdr as an artificial receptor. The change in the absorption peak of its reduced state at 550 nm can be used in indirectly evaluating Fdx activity and evaluating the in vitro coupling effect of Fdx–Fdr on the basis of the electron transfer sequence of coenzyme NADH → Fdr → Fdx → cytochrome C. The mixture was evenly mixed in a 1.5 mL reaction system composed of 200 µL of cytochrome C, 50 µL of 200-fold-diluted purified enzyme solution Fdx–Fdr, 650 µL of PBS buffer with pH 7.2–7.4, 100 µL of 1 mM NaCl solution, and 180 µL of mixture was taken out and added to a 96-well plate, then 20 µL of 30 mM NAD(P)H was added to initiate the electron transfer reaction. The OD_{550} value change within 10 min was immediately measured with a microplate, and the absorption change curve was recorded.

Investigation of the target enzymes in the catalytic reaction of VD_3 hydroxylation

In order to establish the in vitro hydroxylation system of VD_3, a recombination system containing the target proteins (CYP105A1, Fdx–Fdr), $FeCl_3$ (100 mM), glucose (60 mM), and NaCl (50 mM) was initially constructed by adding the corresponding protein solutions. The role of the target proteins in catalyzing VD_3 hydroxylation was explored. The substrate VD_3 was dissolved in dimethyl sulfoxide (DMSO) and eventually added at a concentration of 0.1 mg/mL. Then, 1 mM NAD(P)H was added to initiate the reaction. The hydroxylation reaction (10 mL) was carried out in a constant temperature oscillator at 30 °C and oscillation speed of 180 rpm. After 24 h of reaction, ethyl acetate was added to stop the reaction. The reaction solution was extracted twice with 2 mL of ethyl acetate, and the organic phase was removed with a rotary evaporator. Methanol was added for solubilization and analyzed through high- performance liquid chromatography (HPLC).

HPLC analysis of the VD_3 yield

HPLC is widely used in determining VD_3 and its hydroxylation products (Hayashi et al. 2008, 2016; Sawada et al. 2004; Sugimoto et al. 2008). Given that VD_3 and its hydroxylation products have highly similar structures and hydrophobicity, the condition of HPLC in this study was as follows: mobile phase, methanol/water (95:5, v/v); column, Agilent C18 (4.6 mm × 9 mm × 150 mm) reversed-phase column chromatography silica gel; detection wavelength, 264 nm; flow rate; 1.0 mL/min; injection volume, 20 µL; column temperature, 40 °C.

Construction of a one-bacterium-multi-enzyme system for hydroxylation of VD_3

An expression plasmid for CYP105A1 was constructed. A PCR fragment containing the *CYP105A1* gene with *Bam*HI and *Hin*dIII sites was obtained using the primers CYP105A1-F1 and CYP105A1-R1 (Table 2). The PCR fragment was inserted into the MCS1 of the plasmid pETDuet-1 after double enzyme digestion. The resultant expression plasmid pETDuet-1-*CYP105A1* was introduced into *E. coli* DH5α for preservation and subsequent construction.

An expression plasmid for the co-expression of CYP105A1 and Fdx–Fdr was constructed. The PCR fragment containing *Fdx–Fdr* with *Nde*I and *Xho*I restriction endonuclease sites was obtained using the primers Fdrx–F1and Fdrx–R1 (Table 2). The PCR fragment after double enzyme digestion by *Nde*I and *Xho*I was inserted into the MCS2 of the plasmid pETDuet-1-*CYP105A1*. After verification, the resultant expression plasmid pETDuet-1-*CYP105A1-Fdx-Fdr* was introduced into *E. coli* DH5α for preservation and *E. coli* BL21(DE3) for expression.

Whole-cell conversion of VD_3 to its active forms $25(OH)VD_3$ and $1\alpha, 25(OH)_2VD_3$

For the whole-cell conversion experiments, VD_3 was dissolved in DMSO as a solubilizing agent. A whole-cell catalytic approach was used in verifying the activities of the expressed key enzymes. The hydroxylation efficiency of VD_3 was investigated in terms of co-solvent DMSO, the addition of coenzyme NADH, and loading of biocatalyst. The hydroxylation efficiency of VD_3 catalyzed by the enhanced enzyme CYP105A1 with the assistance of the electron transfer chain Fdx–Fdr was explored.

The hydroxylation activity of recombinant *E. coli* for VD_3 was determined in a 10 mL system. Recombinant cells, PBS buffer (pH7.2–7.4), 0.1 g/L VD_3, and 1 mM coenzyme NADH were added to the reactor. The sample was then subjected to an oscillatory reaction at 30 °C and 180 rpm for 24 h. Ethyl acetate was added to stop the reaction. After the catalysis, ethyl acetate was used for extraction, and the extraction solution was collected, evaporated, and cleaned with a rotary evaporator. After methanol was added and re-dissolved, the solution was filtered with a 0.45 μm aperture filter membrane. The components of the filtrate were analyzed through HPLC.

The effect of the co-solvent DMSO on the hydroxylation efficiency of VD_3 was investigated. The concentration gradient of the co-solvent DMSO (with a volume ratio of 0.1–3%) was set and added to the catalytic system at the same time with the VD_3. Then, the sample was placed at 30 °C and 180 rpm for 24 h of oscillating reaction, and ethyl acetate was added to stop the reaction. After the reaction, the sample was extracted with ethyl acetate, then the extraction solution was collected and evaporated to dryness with a rotary evaporator. After methanol was added and re-dissolved, the components in the sample were analyzed by HPLC.

The effect of NADH addition on the hydroxylation efficiency of VD_3 was studied. Coenzyme NADH (1.0 mM) was added to the 10 mL reaction system. The control group contained no coenzyme NADH, and other conditions remained unchanged.

To investigate the effect of biocatalyst loading (i.e., concentration of bacteria) on the hydroxylation efficiency of VD_3, 5, 10, 15, 25 and 35 g/L of recombinant cells were respectively added to the 10 mL hydroxylation reaction system. Other conditions were unchanged.

Statistical analysis

The experiments were carried out in triplicates, and the results were represented as the mean ± standard deviation. The student's *t* test was used for statistical analysis using SPSS 17.0 software. Graphing of data was performed using Origin 8.5 software.

Results

Soluble expression and purification of the target proteins

In order to study the in vitro hydroxylation capacity of the key proteins, the plasmids pET28a(+)-*CYP105A1* and pET28a(+)-*Fdx-Fdr* for the expression of the target proteins were successfully constructed.

For enhancing the soluble expression of the target proteins CYP105A1, Fdx, and Fdr, the culture condition was set as 24 °C for 24 h. According to SDS-PAGE analysis, the apparent molecular weights of the three proteins were 50.6, 16.0, and 45.0 kDa (Fig. 2), which were consistent with the expected values and indicated that the three proteins were correctly expressed in recombinant strains *E. coli* BL21/pET28a(+)–*CYP105A1* and *E. coli* BL21/pET28a(+)–*Fdx–Fdr*. The intracellular proteins in recombinant strains were released through ultrasonic crushing followed by Ni^{2+}-NTA column purification and SDS–PAGE analysis. As shown in Fig. 2, after Ni^{2+}-NTA column purification, single protein bands were obtained for all the three target proteins, indicating that the target proteins were successfully purified.

Biological activity analysis of the electron transport chain

The purified proteins were further used in analyzing the biological activity of the electron transport chain. First, the electron transfer effect of Fdr was evaluated. The OD_{600} values in the sample without NAD(P)H were stable and almost unchanged, whereas those in the two groups with the coenzyme NAD(P)H decreased. This result indicated that the electron transport chain Fdx–Fdr can effectively receive the coenzyme NAD(P)H (Fig. 3a). The OD_{600} reduction rate of the sample with coenzyme NADH was quicker than that of the coenzyme NADPH group, suggesting that the coenzyme NADH had a stronger ability to reduce Fdr than NADPH and the electron transfer (Fdx–Fdr) prefers coenzyme NADH (Fig. 3a).

Moreover, the oxidative activity of Fdx was assessed. Compared to the control group, the treatment group with coenzyme NAD(P)H showed significantly higher OD_{550} values, demonstrating that Fdx was able to couple with Fdr to transfer electrons from coenzyme NAD(P)H to Fdx via the electron transport chain. An increasing trend was more evident in the treatment with NADH, further indicating that the electron transport chain (Fdx–Fdr) had higher selectivity for coenzyme NADH (Fig. 3b).

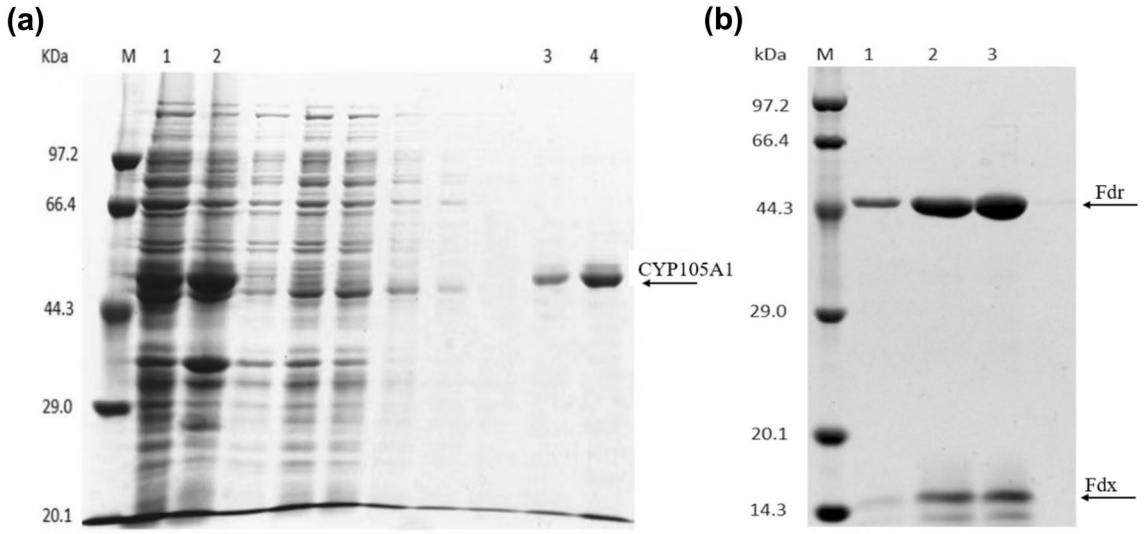

Fig. 2 SDS–PAGE analysis of cytosolic fractions of the recombinant *E. coli* and the purified samples of CYP105A1, Fdx, and Fdr. The molecular weights of CYP105A1, Fdx, and Fdr were approximately 50.6, 16.0, and 45.0 kDa, respectively. **a** Lane M: protein molecular weight marker, Lane 1: proteins in supernatant from *E. coli* BL21/pET28a-CYP105A1 after IPTG induction, Lane 2: precipitated proteins from *E. coli* BL21/pET28a-CYP105A1 after IPTG induction, Lanes 3 and 4: purified CYP105A1 from supernatant. **b** SDS–PAGE analysis of the purified samples of Fdx and Fdr. Lane M: protein molecular weight marker, Lanes 1–3: purified Fdx and Fdr from supernatant

In vitro catalytic study of the VD_3 hydroxylation

After purification using the Ni–NTA column, the hydroxylation reaction system for the synthesis of physiologically active VD_3 was established in vitro and used in verifying the hydroxylation activity of hydroxylase CYP105A1 assisted by the electron transport chain Fdx–Fdr, where NADH was employed as the coenzyme to initiate the hydroxylation reaction.

The analysis of VD_3 and corresponding hydroxylation products through HPLC is shown in Fig. 4. The retention time of the standard samples 25(OH)VD_3 and 1α, $25(OH)_2VD_3$ is respectively 5.147 and 3.857 min (Fig. 4a and b), while the VD_3 hydroxylation products (Fig. 4c) exhibited two peaks with the same retention time with the standard samples 25(OH)VD_3 and 1α, $25(OH)_2VD_3$. This indicated that CYP105A1 could hydroxylate the C25 and C1α sites of VD_3 and convert VD_3 to its active forms, 25(OH)VD_3 and 1α, $25(OH)_2VD_3$, under the combined action of the electron transport chain (Fdx–Fdr).

Determination of the hydroxylation activity of the recombinant *E. coli* for VD_3

The recombinant *E. coli* BL21(DE3)/pETDuet-1-*CYP105A1-Fdx-Fdr* was constructed successfully. The SDS–PAGE results of the three recombinant proteins, CYP105A1, Fdx and Fdr are shown in Fig. 5, indicating that they were correctly expressed in recombinant *E. coli* cells. To verify if the recombinant *E. coli* cells had the hydroxylation function for VD_3, VD_3 and corresponding hydroxylation products were subjected to HPLC analysis. The results showed that the characteristic absorption peaks appeared at corresponding retention times, indicating that the constructed recombinant expression strain had hydroxylation function and could catalyze the hydroxylation reaction of VD_3 to produce two active products: 25(OH)VD_3 and 1α, $25(OH)_2VD_3$. The yield of the product 25(OH)VD_3 was 1.245 ± 0.27 mg/L, whereas that of the product 1α, $25(OH)_2VD_3$ was only 0.192 ± 0.15 mg/L. This result showed that the hydroxylation of VD_3 by hydroxylase CYP105A1 was carried out step by step, and 25(OH)VD_3 served as the intermediate, and 1α, $25(OH)_2VD_3$ served as the final product.

Effect of DMSO concentration on hydroxylation activity

The effect of different concentrations of DMSO on the hydroxylation of VD_3 was investigated (Fig. 6a). The yields of the two active products were significantly different. The product 25(OH)VD_3 had the highest yield, which ranged from 1.377 mg/L to 1.767 mg/L. The highest yield of 1α, $25(OH)_2VD_3$ was only 0.386 mg/L. Although the highest yields of the two products were obtained at 0.1% DMSO concentration, a low DMSO concentration is not conducive to the dissolution of VD_3 and may be detrimental to the yields of the target products during the expanded

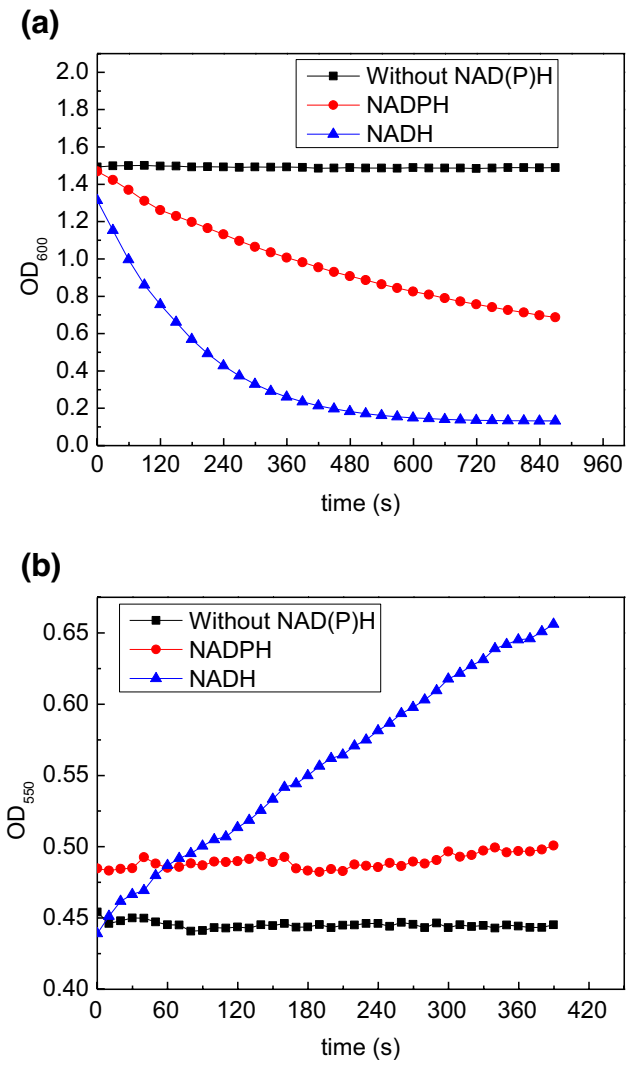

Fig. 3 Study on the coupling activity of electron transport chain. **a** Preference for coenzyme NAD(P)H by electron transfer chain. **b** Changing curve of cytochrome C at OD value of 550 nm

generation process. Therefore, a high concentration of DMSO was used to solubilize the substrate and product and increase the yields of the target products.

When 0.5%–1.5% co-solvent DMSO was added, the yields of the two products were relatively stable, and the highest yield of the final product 1α, $25(OH)_2VD_3$ was obtained at 1% of DMSO, reaching 0.348 mg/L. The yield of $25(OH)VD_3$ reached 1.581 mg/L, which was slightly lower than that of the group with 0.5% addition. When the DMSO concentration was 2%, although 1α, $25(OH)_2VD_3$ was higher than for 1% DMSO addition, the content of $25(OH)VD_3$ was much lower than that after the addition of 1% DMSO. Therefore, given the total yield of both two products, 1% DMSO was selected for the whole-cell catalysis experiments.

Effect of coenzyme NADH addition on the hydroxylation efficiency of VD_3

The effect of NADH addition on hydroxylation efficiency was further investigated according to the optimization of the co-solvent DMSO (Fig. 6b). The recombinant strains themselves produce the coenzyme NADH during metabolism, which can promote the hydroxylation of VD_3 and catalyze the synthesis of physiologically active products $25(OH)VD_3$ and1α, $25(OH)_2VD_3$.

The treatment group with 1 mM coenzyme NADH had 0.660 mg/L $25(OH)VD_3$, and the final product 1α, $25(OH)_2VD_3$ yield was 0.492 mg/L. The treatment group with 1 mM coenzyme NADH had a significantly higher amount of active substance $25(OH)VD_3$ than the control group ($p < 0.05$), but the yield of 1α, $25(OH)_2VD_3$ did not change significantly. This result indicated that the addition of coenzyme NADH increased the hydroxylation efficiency of the C25 site.

Effect of cell concentration on the hydroxylation efficiency of VD_3

The addition of key proteins in the whole-cell catalytic reaction is an important step in the catalytic process, and the addition of proteins is determined by the number of recombinant cells added. Therefore, the effect of the cell concentration on the hydroxylation activity of VD_3 was further investigated on the basis of co-solvent DMSO and NADH concentration (Fig. 6c).

The yields of the two active products gradually increased with the increase in cell concentration. The highest yields were obtained at 35 g/L, where the concentrations of $25(OH)VD_3$ and 1α, $25(OH)_2VD_3$ reached 2.491 and 0.698 mg/L, respectively. As the cell concentration increased further, the viscosity of the reaction solution increased, and the transfer of oxygen was restricted, resulting in insufficient dissolved oxygen in the later stages of the reaction. With further increase in the cell concentration, the yields of both products started to decrease. A final cell concentration of 35 g/L was selected.

Discussion

VD_3 presents as a prohormone in mammals, including humans (Jones et al. 1998). It is not physiologically active by itself, but after conversion by CYP450 enzymes, including CYP105A1, physiologically active $25(OH)VD_3$ and 1α, $25(OH)_2VD_3$ are produced. The former is the predominantly active form, which was supported by the results of this study. Given that 1α, $25(OH)_2VD_3$ is the most active form, how to further improve hydroxylation activity towards the C1α

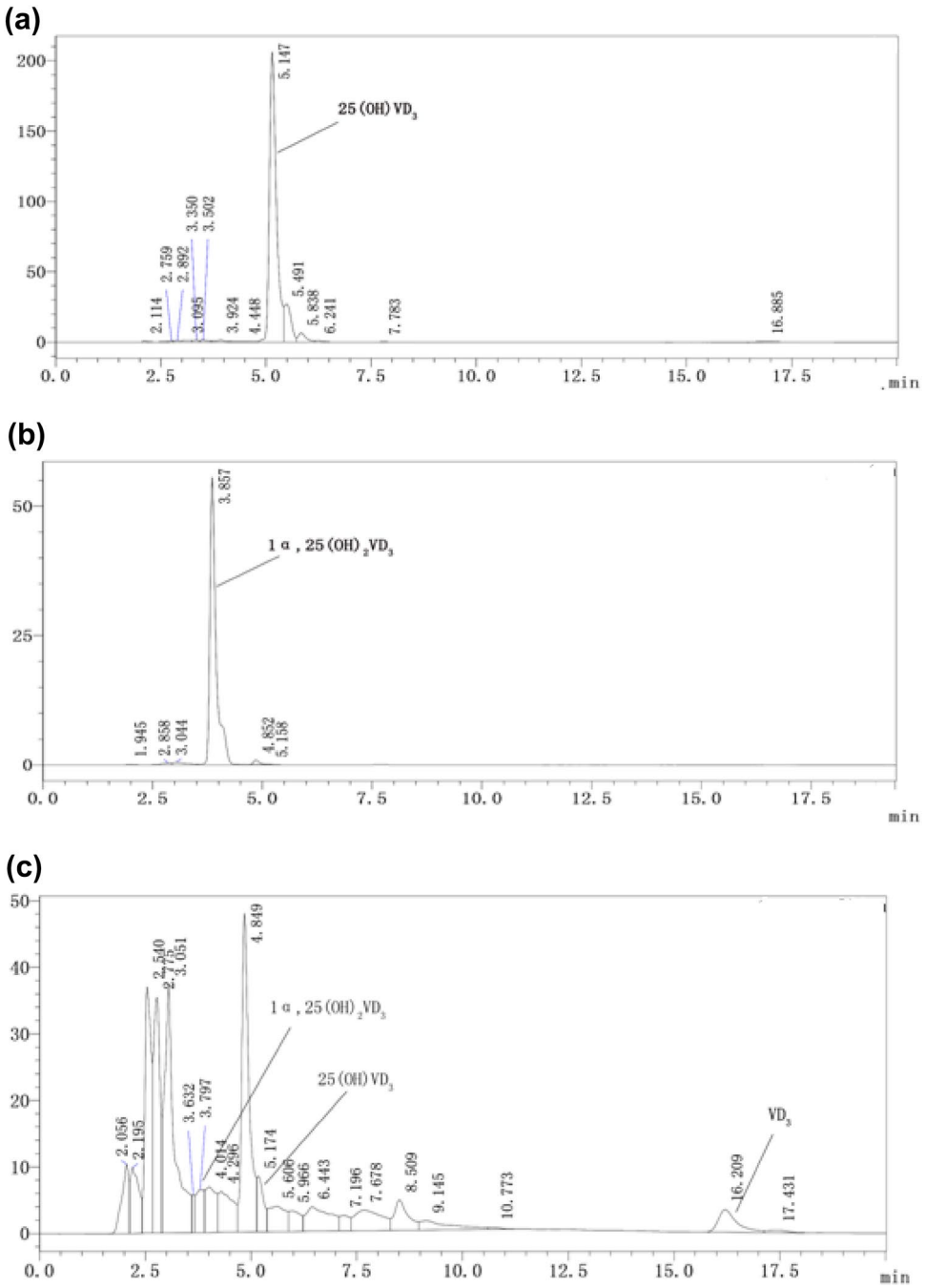

Fig. 4 The analysis of VD_3 and corresponding hydroxylation products through HPLC. **a** HPLC chromatogram of the standard sample 25(OH) VD_3, **b** HPLC chromatogram of the standard sample 1α, $25(OH)_2VD_3$, and **c** HPLC chromatogram of the VD_3 hydroxylation products in vitro

site will be the direction of subsequent research. In terms of molecular manipulation, spatial structure optimization and active site modification may be effective approaches.

Studies on the structure of the CYP105A1 protein have shown that Arg73 and Arg84 are the key residues that maintain its activity and the single and double mutation of R73V/R84A alters substrate preference and enhances hydroxylation activity relative to that of a wild-type enzyme (Hayashi et al. 2008). Hayashi et al. (2016) demonstrated that the R73V/R84A double mutation of CYP105A1 has a hydroxylation capacity not only for VD_3 but also for VD_2 and a double-mutation enzyme has a higher C25 hydroxylation capacity and C26 (C27) hydroxylation activity to VD_2.

A majority of CYP450 enzymes must rely on the coenzyme NAD(P)H to transfer electrons through the electron transport chain and catalyze different chemical reactions (Hannemann et al. 2007). Although the endogenous electron transport chain exists in microorganisms, it may not be sufficient for the large-scale production of active VD_3 with engineered bacteria. The heterologous expression of the electron transport chain can solve the above problems, although a high coupling efficiency of the electron transport chain must

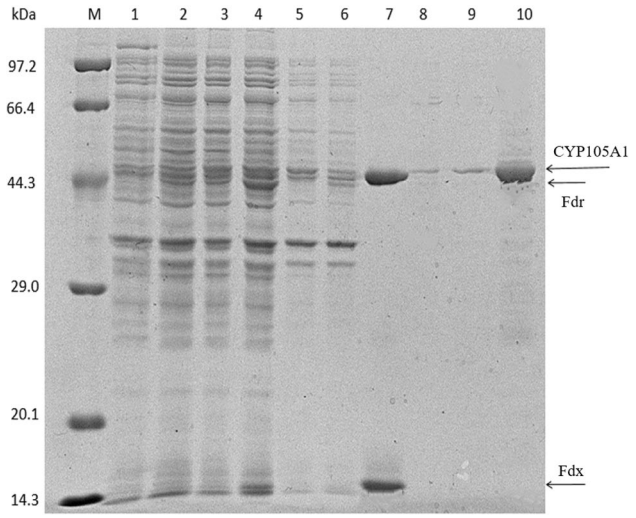

Fig. 5 SDS–PAGE analysis of cytosolic fractions of the recombinant *E. coli*. Lane M: protein molecular weight marker, Lane 1: proteins in supernatant from *E. coli* BL21 after IPTG induction, Lane 2: proteins in supernatant from *E. coli* BL21/pETDuet-1 after IPTG induction, Lane 3: proteins in supernatant from *E. coli* BL21/pETDuet-1-*CYP105A1* after IPTG induction, Lane 4: proteins in supernatant from *E. coli* BL21/pETDuet-1-*CYP105A1-Fdx-Fdr* after IPTG induction, Lane 5: precipitated proteins from *E. coli* BL21/pETDuet-1-CYP105A1 after IPTG induction, Lane 6: precipitated proteins from *E. coli* BL21/pETDuet-1-*CYP105A1-Fdx-Fdr* after IPTG induction, Lane 7: purified Fdx and Fdr, Lane 8–10: purified CYP105A1 from supernatant

be ensured using CYP450 enzymes. Fdx–Fdr can act as an efficient electron donor in *E. coli*, with good coupling to different CYP450 enzymes (Goñi et al. 2009; Ke et al. 2017). The results of the present study verified the above findings. As reported in previous research, the addition amount of Fdr should be limited on a certain scale; otherwise, the activity of CYP105A1 will be inhibited (Sawada et al. 2004).

Given that the coenzyme NAD(P)H produced by the bacterium itself may not be sufficient for the large-scale production of active VD_3, the hydroxylation reaction can be facilitated by the addition of coenzyme NAD(P)H in vitro. It is demonstrated that the enhancement of hydroxylation efficiency by NADH was more obvious than that by NADPH. Although in vitro hydroxylation produces active VD_3, it is difficult to use in the industrial production of active VD_3 in view of cost and efficiency. Therefore, in this study, a one-bacterium-multi-enzyme system was constructed to produce active VD3, but the yield was not high. Hence, the culture conditions will be further optimized in the next step. Given the obvious disadvantages of adding coenzyme NADH in vitro, such as extremely high cost and low stability, we will consider constructing a coenzyme regeneration system in vivo.

In conclusion, a recombinant engineered bacterium containing the hydroxylase gene *CYP105A1* and electron

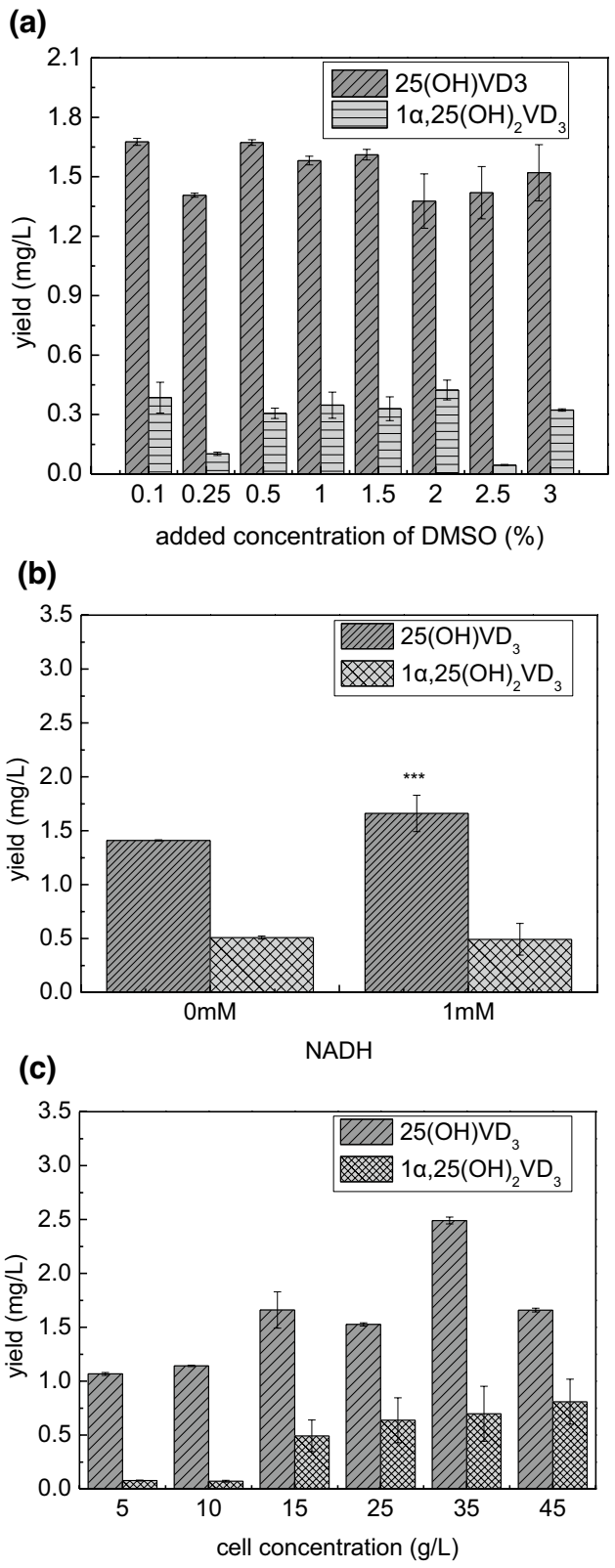

Fig. 6 **a** The effect of different concentrations of DMSO on the hydroxylation efficiency of VD_3; **b** the effect of NADH addition on the hydroxylation efficiency of VD_3; **c** the effect of different concentrations of bacteria on the hydroxylation efficiency of VD_3

transfer chain gene *Fdx–Fdr* was constructed to establish a one-bacterium-multi-enzyme reaction system, which was used to catalyze the hydroxylation of VD_3 by whole cells. The engineered strain with hydroxylation function obtained by genetic engineering catalyzed the synthesis of physiologically active VD_3, and the experiment showed that the construction of the engineered bacteria was successful. Furthermore, the goal of using hydroxylase CYP105A1 to catalyze the synthesis of physiologically active VD_3 was achieved. Hence, this study laid a solid foundation for the industrial production of active VD_3 in future.

Acknowledgements This study was supported by the Natural Science Foundation of Zhejiang Province, China (No. LY21C200006).

Declarations

Conflict of interest The authors declare that they have no competing interests.

Research involving human participants and/or animals This article does not contain any studies with human participants or animals performed by the author.

References

Ahmed SA, Mesbah MK, Youssef DT, Khalifa SI (2014) Microbial production of 1α-hydroxyvitamin D_3 from vitamin D_3. Nat Prod Res 28:444–448

Brenza HL, DeLuca HF (2000) Regulation of 25-hydroxyvitamin D_3 1α-hydroxylase gene expression by parathyroid hormone and 1, 25-dihydroxyvitamin D_3. Arch Biochem Biophys 381:143–152

Bury Y, Ruf D, Carlberg C, Hansen CM, Kissmeyer AM, Binderup L (2001) Molecular evaluation of vitamin D_3 receptor agonists designed for topical treatment of skin diseases. J Invest Dermatol 116:785–792

Dean RL, Pocock T (2004) Diphenyl carbazide restores electron transport in isolated, illuminated chloroplasts after electron transport from water has been eliminated by mild heat treatment. Biochem Mol Biol Edu 32:381–389

DeLuca H (1982) Metabolism and molecular mechanism of action of vitamin D: 1981. Biochem Soc Transact 10:147–158

DeLuca HF, Schnoes HK (1983) Vitamin D: recent advances. Annu Rev Biochem 52:411–439

Fujii Y, Kabumoto H, Nishimura K, Fujii T, Yanai S, Takeda K, Tamura N, Arisawa A, Tamura T (2009) Purification, characterization, and directed evolution study of a vitamin D_3 hydroxylase from *Pseudonocardia autotrophica*. Biochem Biophys Res Commu 385:170–175

Goñi G, Zöllner A, Lisurek M, Velázquez-Campoy A, Pinto S, Gómez-Moreno C, Hannemann F, Bernhardt R, Medina M (2009) Cyanobacterial electron carrier proteins as electron donors to CYP106A2 from *Bacillus megaterium* ATCC 13368. Biochim Biophys Acta BBA 1794:1635–1642

Hannemann F, Bichet A, Ewen KM, Bernhardt R (2007) Cytochrome P450 systems—biological variations of electron transport chains. Biochim Biophys Acta BBA 1770:330–344

Hayashi K, Sugimoto H, Shinkyo R, Yamada M, Ikeda S, Ikushiro S, Kamakura M, Shiro Y, Sakaki T (2008) Structure-based design of a highly active vitamin D hydroxylase from *Streptomyces griseolus* CYP105A1. Biochemistry 47:11964–11972

Hayashi K, Yasuda K, Yogo Y, Takita T, Yasukawa K, Ohta M, Kamakura M, Ikushiro S, Sakaki T (2016) Sequential hydroxylation of vitamin D_2 by a genetically engineered CYP105A1. Biochem Biophys Res Commu 473:853–858

Hefti MH, Dixon R, Vervoort J (2001) A novel purification method for histidine- tagged proteins containing a thrombin cleavage site. Anal Biochem 295:180–185

Imoto N, Nishioka T, Tamura T (2011) Permeabilization induced by lipid II-targeting lantibiotic nisin and its effect on the bioconversion of vitamin D_3 to 25-hydroxyvitamin D_3 by *Rhodococcus erythropolis*. Biochem Biophys Res Commu 405:393–398

Janknecht R, de Martynoff G, Lou J, Hipskind RA, Nordheim A, Stunnenberg HG (1991) Rapid and efficient purification of native histidine-tagged protein expressed by recombinant vaccinia virus. Proc Natl Acad Sci USA 88:8972–8976

Jones G, Strugnell SA, DeLuca HF (1998) Current understanding of the molecular actions of vitamin D. Physiol Rev 18:73–89

Kametani T, Furuyama H (1987) Synthesis of vitamin D_3 and related compounds. Med Res Rev 7:147–171

Kang DJ, Im JH, Kang JH, Kim KH (2015) Whole cell bioconversion of vitamin D_3 to calcitriol using *Pseudonocardia* sp. KCTC 1029BP. Bioproc Biosyst Eng 38:1281–1290

Kang DJ, Lee HS, Park JT, Bang JS, Hong SK, Kim TY (2006) Optimization of culture conditions for the bioconversion of vitamin D_3 to 1α, 25-dihydroxyvitamin D_3 using *Pseudonocardia autotrophica* ID 9302. Biotechnol Bioproc Eng 11:408–413

Kawauchi H, Sasaki J, Adachi T, Hanada K, Beppu T, Horinouchi S (1994) Cloning and nucleotide sequence of a bacterial cytochrome P-450VD_{25} gene encoding vitamin D-3 25-hydroxylase. Biochim Biophys Acta BBA 1219:179–183

Ke X, Ding GJ, Ma BX, Liu ZQ, Zhang JF, Zheng YG (2017) Characterization of a novel CYP51 from *Rhodococcus triatomae* and its NADH-ferredoxin reductase-coupled application in lanosterol 14α-demethylation. Process Biochem 62:59–68

Koyama T, Shibakura M, Ohsawa M, Kamiyama R, Hirosawa S (1998) Anticoagulant effects of 1α, 25-dihydroxyvitamin D_3 on human myelogenous leukemia cells and monocytes. Blood J Am Soc Hematol 92:160–167

Luo J, Jiang F, Fang W, Lu Q (2017) Optimization of bioconversion conditions for vitamin D_3 to 25-hydroxyvitamin D using *Pseudonocardia autotrophica* CGMCC5098. Biocatal Biotransform 35:11–18

Pham SQ, Gao P, Li Z (2013) Engineering of recombinant *E. coli* cells co-expressing P450pyrTM monooxygenase and glucose dehydrogenase for highly regio- and stereoselective hydroxylation of alicycles with cofactor recycling. Biotechnol Bioeng 110:363–373

Pike JW (1991) Vitamin D_3 receptors: structure and function in transcription. Annu Rev Nutr 11:189–216

Sakaki T, Sugimoto H, Hayashi K, Yasuda K, Munetsuna E, Kamakura M, Ikushiro S, Shiro Y (2011) Bioconversion of vitamin D to its active form by bacterial or mammalian cytochrome P450. Biochim Biophys Acta BBA 1814:249–256

Sasaki J, Mikami A, Mizoue K, Omura S (1991) Transformation of 25- and 1 alpha-hydroxyvitamin D3 to 1 alpha, 25-dihydroxyvitamin D_3 by using *Streptomyces* sp. strains. Appl Environ Microbiol 57:2841–2846

Sawada N, Sakaki T, Yoneda S, Kusudo T, Shinkyo R, Ohta M, Inouye K (2004) Conversion of vitamin D_3 to 1α, 25-dihydroxyvitamin D_3 by *Streptomyces griseolus* cytochrome P450SU-1. Biochem Biophys Res Commu 320:156–164

Sugimoto H, Shinkyo R, Hayashi K, Yoneda S, Yamada M, Kamakura M, Ikushiro SI, Shiro Y, Sakaki T (2008) Crystal structure of CYP105A1 (P450SU-1) in complex with 1α, 25-dihydroxyvitamin D_3. Biochemistry 47:4017–4027